**Article:**
Hopkinson, N., Haworth, B. and Hitt, D.J. (2011) Fracture Mechanics Approach to compare Laser Sintered parts and Injection Mouldings of Nylon-12. Proceedings of the Institution of Mechanical Engineers, Part B: Journal of Engineering Manufacture, 225 (9). 1663 - 1672. ISSN 0954-4054

https://doi.org/10.1177/0954405411402141

# FRACTURE MECHANICS APPROACH TO COMPARE LASER SINTERED PARTS AND INJECTION MOULDINGS OF NYLON-12

**DJ Hitt [1], B Haworth [1] and N Hopkinson [2]**

[1] Department of Materials, Loughborough University, UK.

[2] Wolfson School of Mechanical and Manufacturing Engineering, Loughborough University, UK.

## Abstract:

In comparison to equivalent parts made by injection moulding (IM), components manufactured by laser sintering (LS) are often perceived to offer inferior mechanical properties, yet the evidence for this is rarely based upon systematic research studies. In this paper, attempts have been made to conduct a fundamental study of the fracture behaviour of both injection moulded and laser sintered parts, based upon a modification of a standard technique used to determine linear elastic fracture mechanics (LEFM) parameters. The influence of specimen thickness (in the range 2-10mm) was also included in the experimental plan, which was concentrated upon the testing of single edge notch bending (SENB) beam specimens.

Force-displacement characteristics demonstrated significant plastic deformation in nylon (PA12) specimens, so that the J-integral method was used to obtain quantitative fracture parameters, including the energy requirements for crack growth. Comparisons of this parameter showed thickness dependent, 'geometry-sensitive' data for each set of samples. For the injection moulded SENB specimens, energy absorption decreased with increasing thickness, a result attributed to the influence of plane strain dominated conditions. In contrast, laser sintered samples exhibited increased toughness as specimen thickness increased towards 10mm; this could not be explained by density or particle melting data and may be interpreted by changes in molecular structure that occur during the additive manufacturing process.

**Keywords: fracture toughness, nylon-12, laser sintered, injection moulded**

## INTRODUCTION

Nylon 12 powders for laser sintering have a crystalline melting endotherm with a peak around 190°C. When such powders are used in additive manufacturing the bed temperature is maintained at ~172°C which means that after the laser has traversed the bed, the freshly sintered layer will have been heated to over 190°C and will subsequently cool back to the bed temperature. Now, if the temperature of that layer remains above the bed temperature (before the next powder layer is applied) the temperature of the new layer will be closer to the melt temperature, enabling the new layer to be sintered more effectively. From this it would reasonable to expect that as part thickness increases, the heat retention by the part during sintering will increase, such that sintering efficiency will improve leading to enhanced mechanical properties.

Laser sintered components made from nylon-12 are known to have a level of porosity and when tested to break tend to fail in a brittle manner: in tensile testing, standard sintered specimens typically show elongation at break values of 5-20% [1,2]. These physical properties indicate that under the standard regime of testing and analysis defined in fracture toughness standards, laser sintering parts of different thickness would fail in the requisite brittle manner offering a rigorous examination of the effect of sample thickness. A key factor that can influence the properties of laser sintered components is the degree of particle melt. This can be determined by Differential Scanning Calorimetry (DSC) [3]: a DSC trace of a sample of nylon-12 powder prior to sintering will usually show a single melt peak at ~190°C. If full melting of the powder occurs during the sintering process then a sample cut from the sintered part will show a single melt peak at ~180°C. However, if the laser energy is insufficient for full melting the DSC trace will show a double melt peak: one at ~180°C corresponding to the material melted during sintering and a second peak towards 190°C due to unmelted material. The latter peak is usually much smaller, indicating that most of the material has melted.

Engineering plastics components manufactured by conventional processes such as extrusion or injection moulding are usually associated with a high degree of accuracy and consistency, but are prone to property variations caused by molecular orientation, residual stress and structural irregularity due to inhomogeneous cooling rates through the thickness of the part. Furthermore, attempts to measure the toughness of injection moulded parts by fracture mechanics are made more complex by the sensitivity to specimen thickness. As thickness increases, contributions to energy absorption by yielding at the crack tip are suppressed by the dominance of plane strain conditions throughout the majority of the sample; consequently, failure by crack

growth occurs and macroscopic brittle fracture becomes more likely, resulting in a decrease in measured fracture parameters towards limiting, plane strain dominated values [4].

The objective of this study was to employ a systematic and more fundamental fracture mechanics approach to compare the properties of laser sintered and injection moulded PA12 parts, investigating the effects of specimen thickness, to further understand the influence of different thermo-mechanical history on the toughness of components manufactured by different routes.

## 2. EXPERIMENTAL

### 2.1. Preparation of Test Specimens

A Negri-Bossi NB62 injection moulding machine was employed to prepare specimens from a grade of nylon-12 supplied by Arkema: Rilsan AMNO (melt temperature of 179°C). A mould with a single, rectangular-section cavity (length 125mm, width 15mm and depth 10mm) was used. The melt was injected at 240°C into the mould, which was controlled at 40°C. To produce a range of specimen thicknesses the mould cavity was fitted with a series of uniform steel spacers of increasing thickness. As the spacer thickness increased the shot size was adjusted accordingly to produce parts with typical (nominal) thicknesses of 10.1mm (no spacer), 8.3mm, 6.2mm, 4.2mm and 2.2mm. However, a degree of mould shrinkage occurred which meant that the parts were slightly 'waisted'; i.e, the actual thickness was lower towards the centre of the 15mm width than at the edges (where the stated values were measured).

Laser sintered parts were produced using an EOS Formiga P100 machine. The nylon-12 powder was PA2200 (melt temperature of 187°C), supplied by EOS (Munich, Germany). The material feed to the machine was a 50:50 mix of virgin and used powders: the latter being unsintered powder that has been recovered from a previous laser sintering process. This is normal practice for laser sintering for two reasons: it reduces material wastage and improves mechanical properties of laser sintered products [5]. The build parameters employed are listed in Table 1. By convention, in laser sintering, the x-axis and y-axis of the build chamber are respectively parallel and perpendicular to the front face of the machine and the z-axis is the vertical direction in which powder layers are added. The set of laser sintered parts measured 125mm in the x-direction and 15mm in the y-direction. The thicknesses in the z-direction were typically 2.3mm, 4.3mm,

6.3mm, 8.3mm and 10.2mm. For convenience, nominal thickness values of 2, 4, 6, 8 and 10mm are used elsewhere in the text.

## 2.2. Three point bend testing - fracture mechanics

Both injection moulded and laser sintered parts were prepared for testing under single edge notch bending (SENB) conditions according to the relevant standards [6, 7]. A v-notch was cut into the specimen at its centre point and a natural, 'dead sharp' crack was added at the tip of the v-notch using a sharp razor blade. Thus, as illustrated in Figure 1, the initial total notch depth is "a". A Tinius Olsen HK50 tensometer, fitted with a 5kN load cell, was used for the three point bend tests. The two specimen supports were separated by 60mm (that is, 4w) and the loading point was applied to the specimen (directly behind the tip of the crack) at 10mm/min. The test temperature was 22°C. No valid results were obtained with the 2mm thick specimens as these deflected laterally under loading and fell off the supports. Force-displacement curves were obtained for specimens produced by each process, at all the other thicknesses: 4mm, 6mm, 8mm and 10mm. Four injection moulded specimens and four laser sintered specimens of each thickness were tested. In all tests, a detect break criterion of 50% of peak force was used.

The SENB method also requires the extent by which the two specimen supports and the loading point indent into the specimen to be determined so that the force-displacement curve can be corrected [6, 7]. To do this, additional tests were performed at 1mm/min on specimens without notches and with the specimen supports closed to the minimum possible separation. For each thickness, these tests were terminated once the measured force exceeded the maximum force recorded in the tests on notched samples. At each thickness, for both product types, four correction curves were obtained and combined to produce an average curve.

## 2.3. DSC analysis of laser sintered parts.

A TA Instruments series 2010 thermal analyser fitted with a DSC cell was used to determine the melt temperature and melt enthalpy of samples cut from laser sintered specimens. Samples of ~6mg were heated in the DSC cell from 25°C to 215°C at rate of 10°C/min.

## 3. RESULTS

### 3.1. Analysis of raw data - three point bend force displacement curves

A typical force displacement curve for a SLS specimen is shown in Figure 2. Initially, there is a linear elastic response between force and displacement followed by a non-linear region, then plastic deformation by ductile yielding: as this progressed, the force reached a maximum and then fell until the end of the test. Unexpectedly, none of the SLS specimens fractured during a test. In every case, after the peak force had been passed the specimen continued to deflect until the force had fallen to 50% of the measured maximum (this can be seen in Figure 2). The force-displacement response of injection moulded specimens was similar, except that the majority did fracture soon after the force passed through its maximum value.

### 3.2. Fracture analysis

As both product types displayed considerable ductile deformation, analysis by linear elastic fracture mechanics (LEFM) could not be used as this method requires the samples to fail in brittle manner [6]. However, ASTM D 6068-96: 2002 [7] employs a J-integral method whereby force-displacement curves of the nature of those in Figure 2 can be used to obtain fracture toughness values. Essentially, specimens are deflected to a series of fixed displacements without fracture and in each case the total area under the force displacement curve, energy (U) is calculated. The specimens are subsequently broken to enable the dimensions of the plastic deformation zone ($\Delta a$) in the ligament to be measured accurately. The energy values are then plotted against $\Delta a$ to determine a critical strain energy release rate.

A method of analysis drawing upon the procedure defined in ASTM D 6068-96: 2002 [7] has been adopted to derive a single value from the curves for both laser sintered and injection moulded specimens in this study. The method is illustrated in Figure 2 and seeks to determine the energy under the curve up to the end of the elastic response: this can also be considered as the energy to initiate crack growth. This approach is not as rigorous as that of the fracture toughness standards, however, it does offer a means to compare the two specimen types.

In Figure 2 the 'corrected curve' is a plot of force against corrected displacement (ie, the raw data curve displacement minus the correction curve displacement at the same force). A line (S1) defining the slope of the linear response of the corrected curve is then determined. To obtain a clearly defined end point of the elastic portion of the curve the gradient of line S1 is then multiplied by 0.95 and a second line (S2) is constructed with the lower gradient. In Figure 2 this is shown to intersect the corrected curve at point P1. The energy under the corrected curve (U) up to point P1 is then calculated.

The energy, J, to initiate crack growth is calculated from $J = 2U / [h(w-a)]$, in which h is the sample thickness and (w-a) is the ligament behind the tip of the crack. Thickness values were determined for each laser sintered specimen prior to testing, while ligament dimensions, of both product types were measured afterwards. Specimens that had not fractured into two segments during testing were broken afterwards to enable the original ligament dimension to be measured. As the position at which crack growth was initiated was clearly visible by optical microscopy, a travelling microscope was therefore used to measure the ligament in both segments of a specimen and an average value was determined. Ligament dimensions ranged from 6.3-7.0mm for laser sintered specimens and from 7.2-7.5mm for injection moulded. The thickness of injection moulded samples was also determined after testing as it was then easier to measure this at points across the sample width and then calculate an average value to take into account the effect of mould shrinkage.

Overall results for the two specimen types are shown in Figure 3. At the various thicknesses for each specimen type average values of energy to initiate crack growth have been calculated. The error bars represent the standard deviations of the calculated average values. Very distinctive behaviour is evident for the two types of specimen. For injection moulded specimens, there is a decrease in energy absorbed as the specimen thickness increases, from a maximum of 3.7 $kJ/m^2$ (4mm nominal) to 2.7 $kJ/m^2$ (10mm nominal). However, the opposite trend occurs with laser sintered specimens with energy absorbed increasing from 2.9 $kJ/m^2$ to 4.3 $kJ/m^2$ over the same thickness range.

## 3.3. DSC analysis of sintered parts

For DSC analysis cross-sections were cut from laser sintered specimens of all five thicknesses. Two patterns of sampling were adopted. For thicknesses of 2mm and 4mm, samples were taken at the positions shown in

Figure 4(a) and for thicker sections of 6mm, 8mm and 10mm, samples were taken at the positions shown in Figure 4(b). To illustrate the results obtained, DSC curves and melt enthalpies are reported for samples of the two extreme thicknesses, ie, 2mm and 10mm. DSC curves corresponding to all four sample positions in the 2mm part are shown in Figure 5(a). As very similar DSC curves were obtained for sample positions 1 to 9 of the 10mm part only a selection of curves need to be shown here. Curves for sample positions 3, 6 and 9 are shown in Figure 5(b) along with the curve for sample position 10.

It is apparent that a very high degree of particle melting was obtained during the sintering of the two parts as the DSC curves for samples A, B and C in Figure 5(a) and samples 3, 6 and 9 in Figure 5(b) all show a single melt peak [3]. The slight inflection in the melt peak at 190°C of sample D (Figure 5(a)) and the small shoulder in the melt peak, at the same temperature, of sample 10 (Figure 5(b)) reflects the fact that both these samples included some of the surface of the respective sintered parts, where the degree of particle melt will be lower than in the centre. The melt enthalpy for each sample was then determined; the data are presented in Table 2.

Table 2 shows that overall melt enthalpy values ranged from 79J/g to 88J/g with slightly higher values obtained from specimens of greater thickness. DSC analysis of samples taken from sections through the other three specimen thicknesses (4mm, 6mm and 8mm) produced comparable ranges of melt enthalpies to those given in Table 2. Again, melt peaks only showed an inflection or a shoulder at the high temperature end, if the DSC sample included some of the surface of the laser sintered specimen.

## 4. DISCUSSION

The purpose of fracture toughness testing of a material is to determine a 'worst case' failure scenario, that is, to evaluate the minimum stress required to produce crack growth in specimens with pre-existing defects. Toughness of materials is often expressed in terms of the energy requirements to produce new fracture surfaces, as the crack grows towards the critical condition for fracture. Knowledge of fracture properties thus provides designers with a level of certainty regarding the use of a material for a product, especially if the product will have to sustain sudden or prolonged loading. The linear elastic approach to fracture in plastics demands that samples fail in a brittle manner, under testing at 23°C. However, should that not occur then the

test temperature should be reduced, or test velocity increased to ensure that the mode of fracture complies with the failure criteria.

Initially, it was thought that the nature of laser sintered specimens would comply at 23°C, however, the results have shown otherwise. Under the reported test set-up, laser sintered specimens showed considerable plastic deformation which contravened the linear elastic approach. At this point it is worth stressing that the aim of this work was to assess how laser sintered parts of varying thickness performed in comparison with injection moulded under the same test regime. Thus, rather than pursue the low temperature or high test velocity options at that stage, the data that had been generated was analysed using a method based on an ASTM standard. This approach has produced for each material, a measure of 'energy to initiate crack growth' (by plastic deformation) as a function of specimen thickness.

**Force displacement curves for both types of nylon-12 specimen**

Figure 3 shows that as sample thickness increases the energy falls for injection moulded but increases for laser sintered specimens. An explanation of the difference between the two specimen types begins by examining the corrected force displacement curves. Truncated curves are shown in Figures 6(a) and 6(b) for injection moulded and laser sintered respectively. For each curve a short vertical line has been added to mark the intersection of its "S2 line" (defined in Figure 3). It can be seen that for the injection moulded curves the intercept occurs at a lower displacement as the thickness increases, whereas the opposite occurs with the laser sintered curves. It is well known that as thickness increases, plane strain conditions dominate the overall fracture mechanism so that the plastic deformation zone has a diminishing influence on energy absorption and geometry independent fracture parameters can be achieved [4]. This would appear to be consistent with results from the injection moulded specimens, for which it can be argued that as the thickness increases the specimens better satisfy the requirements of fracture toughness criteria and the energy to initiate crack growth falls, possibly towards a limiting value. However, as contrary behaviour occurs in the laser sintered specimens then another factor must be involved to generate the observed increase in energy to initiate crack growth as thickness increases.

For laser sintered materials other possible influential factors could be porosity/density, degree of particle melt, increase in crystallinity or changes in molecular weight/structure. These are now considered in relation

to the premise at the outset of the paper: does increasing thickness of laser sintered nylon-12 specimens mean better sintering through changes in thermal history ?

**Density and porosity**

A measure of the density of the laser sintered specimens was made at each thickness. Samples of known dimensions were weighed, from which apparent densities were calculated. These densities are given in Table 3 and are reasonable as EOS quote a density of 0.93g/cm$^3$ for laser sintered parts produced from their PA2200 nylon-12 material [8]. Taking the maximum density of nylon-12 as 1.020g/cm$^3$ [9], porosity values were calculated by expressing the difference between maximum and apparent densities as a percentage of the maximum. These porosities are given in Table 3. However, in practice the actual relationship between density and porosity can be quite different. Ajoku [10] used an optical microscopy technique to measure the porosity of laser sintered nylon-12 parts and reported values of 1.5-1.9% for densities ranging from 0.91-0.95 g/cm$^3$.

It has been shown that the density, and the mechanical properties, of laser sintered nylon-12 parts increase with laser power [10, 11]. As laser power increases, melt temperature is raised, viscosity would be expected to reduce, and improved melt flow leads to more effective sintering and higher densification. There is a limitation to this process, ie, if the laser energy is too high then degradation of the polymer occurs. The increase in density (and reduction in porosity), shown by Table 3, over the thickness range, indicates better sintering. However, as laser power remained constant for these specimens, it seems very likely that improved heat retention by thicker specimens during sintering effectively raises the melt temperature and as a result, density increases with thickness. However, as the change in density at 4mm thickness to that at 10mm is marginal it is unlikely that this is the sole reason for the trend in the fracture behaviour seen in Figure 3.

**Degree of particle melt and crystallinity**

Figures 5(a) and 5(b) clearly show that a high degree of particle melt is seen in both 2mm and 10mm thick laser sintered specimens. Also, the melt enthalpy values listed in Table 1 are generally higher at the 10mm thickness. However, the overall difference is marginal as averages for the two sets of numbers are 84.6J/g

(10mm) and 82.0J/g (2mm). This suggests that during recrystallisation from the melt the 10mm part cooled at a slower rate to give the slightly higher level of crystallinity. Whilst increased crystallinity will increase mechanical properties it is unlikely that this small difference would have a highly significant effect.

**Molecular weight**

As changes in density and crystallinity are both limited over the thickness range evaluated it would appear that changes in molecular weight in the laser sintered specimens is an additional explanation for the observed changes in energy to initiate crack growth.

The powder feed to the sintering machine comprised 50% virgin powder and 50% used powder. During the sintering process, the latter powder will encounter conditions that meet the criteria for solid state polymerisation of nylon-12 [9, 12]. The requirements are heating in an inert atmosphere, for several hours, at a temperature below, but close to the melt temperature of the polymer. Under these conditions the polymer chains end-link by a condensation reaction and the molecular weight increases.

The change in molecular weight through solid state polymerisation can be substantial. Samples of the virgin nylon-12 powder employed in this study and of a typical used nylon-12 powder recovered from a build have been analysed by GPC [13]. The virgin powder had number average and weight molecular weights of 6,200 and 18,900 g/mol. respectively, compared to 12,600 and 58,100 for the used powder. (Note: the Rilsan injection moulded grade of material had very similar molecular weights to that of the virgin powder.) This means that the used powder has a higher viscosity and may sinter at a different rate to the virgin powder, under given conditions. However, there is plenty of evidence to show that inclusion of used powder in the feed is advantageous in terms of mechanical properties.

Davis et al [14] examined the effect of repeated recycling of nylon-12 powder through a series of laser sintering builds in which the same sintering conditions were applied. An initial build produced standard sized tensile specimens from virgin powder. The used powder was recovered and recycled as the feed for a second build of tensile specimens. After this build the used powder was recycled into a further build and so on, until the powder recovered was insufficient for a viable build. After the fifth build the mass flow rate of the used powder had decreased to ~21g/10minutes, from ~52g/10minutes for the virgin material, reflecting a

significant increase in viscosity through increase in molecular weight. After each build the tensile specimens were tested. After the fifth build, tensile strength had essentially remained constant, while elongation at break had improved significantly, indicating increased ductility for specimens built from higher molecular weight powder.

In the study reported here, if an increase in molecular weight is to account for the observed change in fracture behaviour then some degree of polymerisation would have to occur in the melt state because of the temperatures involved in the process. During sintering of a specimen the laser heats the nylon-12 into the melt state. After sintering, the melt temperature falls back to the bed temperature of 172°C, and as this remains well above the recrystallisation temperature of nylon-12, typically ~150°C [3], the specimen will remain in the melt state until the whole build is complete and is then allowed to cool. Under these conditions, for fixed laser power, it would be necessary for thicker samples to retain more heat during sintering (and cool more slowly back to the bed temperature) to generate the required increase in molecular weight. However, the change in density with thickness suggests the effect of heat retention is limited. Increase in molecular weight in the melt is a viable possibility. Aharoni [9] outlined a procedure by which the molecular weight of nylon-12 could be increased significantly by further melt processing: at temperatures around 300°C the change was achieved in minutes, rather than the hours required for solid state polymerisation.

The results reported in the present study and the subsequent discussion have demonstrated the need for a greater understanding of the molecular weight of laser sintered specimens prepared from nylon-12, in order to explain the observed relationships between mechanical properties and thermo-mechanical history during laser sintering. This is currently the subject of ongoing research activity.

## 5. CONCLUSIONS

Measurements of the fracture behaviour of single edge notched bending (SENB) specimens fabricated by laser sintering and by injection moulding has been obtained, using a technique modified from existing standard methods. The two specimen types show very different behaviour with increasing specimen thickness: energy to initiate crack growth decreases for injection moulded, but increases for laser sintered samples. Whilst the behaviour of injection moulded samples is anticipated, the trend for laser sintered components could be attributed to more effective sintering, as thickness increases. However, two properties

that are indicative of improved sintering, density and degree of particle melt, show very little change with increased thickness. It is suggested that changes in molecular weight, while sintered specimens are held in the melt state, could account for the observed changes in fracture behaviour with thickness. Whether this occurs, and to what extent, would appear to be essential to understanding the properties of laser sintered specimens as a function of thickness and process history.

## ACKNOWLEDGEMENT

This work was supported by EPSRC/IMCRC project 251.

## REFERENCES


1. **Ajoku, U., Saleh, N., Hopkinson, N., Hague R.,** and **Erasenthiram P.** Investigating mechanical anisotropy and end-of-vector effect in laser-sintered nylon parts. *Proc. ImechE, Part B: J. Engineering Manufacture*, 2006, **220**, 1077-1086.

2. **Zarringhalam, H.** Investigation into crystallinity and degree of particle melt in selective laser sintering. PhD Thesis, Loughborough University, 2007.

3. **Zarringhalam, H., Majewski, C.,** and **Hopkinson, N.** Degree of particle melt in Nylon-12 selective laser-sintered parts. *Rapid Prototyping Journal*, 2009, **15(2)**, 126-132.

4. **Williams, J. G.** Fracture Mechanics of Polymers. Ellis Horwood, Chichester, 1984.

5. **Hopkinson, N., Hague R. J. M.,** and **Dickens, P. M.,** Rapid Manufacturing - An Industrial Revolution for the Digital Age, John Wiley & Sons Ltd (England), 2006.

6. **BS ISO 13586:2000.** Plastics - Determination of fracture toughness ($G_{IC}$ and $K_{IC}$) - Linear elastic fracture mechanics (LEFM) approach.

7. **ASTM D 6068-96:2002.** Standard Test Method for Determining J-R Curves of Plastic Materials

8. **EOS Material Data Sheet for PA2200**, 2009.

9. **Aharoni, S. M.** n-Nylons: Their Synthesis, Structure, and Properties. John Wiley & Sons, 1997.

10. **Ajoku, U.** Investigating the compression properties of selective laser sintered nylon-12. PhD Thesis, Loughborough University, 2008.

11. **Caulfield, B., Hugh P. E.,** and **Lohfeld, S.** Dependence of mechanical properties of polyamide components on build parameters in the SLS process. *Journal of Materials Processing Technology*, 2007, **182**, 477-488.

12. **Vouyiouka, S.N., Karatatsani, E. K.,** and **Papaspyrides, C. D.** Solid state polymerisation. *Progress in Polymer Science*, 2005, **30**, 10-37.

13. **RAPRA Technical Report CTR 50056.** Comparison of molecular weight distribution of polyamide samples using conventional gel permeation chromatography. Prepared by S Holding and T Forsyth, May 2009.

14. **Davis, K. R., Gornet, T. J.,** and **Richardson, K. M.,** Material testing method for process control of direct manufacturing in the SLS process. Proceedings of the First International Conference: Advanced Research in Virtual and Rapid Prototyping, Leiria, Portugal, October 2003.

# TABLES

**Table 1: Build parameters**

| | | |
|---|---|---|
| Scan spacing | 0.25 | mm |
| Laser fill power: contours | 21 | W |
| Laser fill power: hatching | 16 | W |
| Scan speed: contours | 2.5 | m $s^{-1}$ |
| Scan speed: hatching | 1.5 | m $s^{-1}$ |
| Process chamber (bed) temperature | 172 | ℃ |

**Table 2: Melt enthalpy values of laser sintered samples**

| | | | | |
|---|---|---|---|---|
| **2mm thick sample:** | | | | |
| Position in Figure 4(a): Melt enthalpy (J/g) | A: 81.7 | B: 81.4 | D: 85.6 | C: 79.1 |
| **10mm thick sample:** | | | | |
| Position in Figure 4(b): Melt enthalpy (J/g) | 1: 87.1 | 2: 85.7 | | 3: 82.7 |
| | 4: 88.0 | 5: 88.0 | | 6: 86.2 |
| | 7: 78.9 | 8: 81.8 | | 9: 86.7 |
| | | | | 10: 81.0 |

**Table 3: Apparent density at each specimen thickness**

| | | | | | |
|---|---|---|---|---|---|
| Nominal thickness (mm) | 2 | 4 | 6 | 8 | 10 |
| Apparent density (g/$cm^3$) | 0.909 | 0.947 | 0.957 | 0.958 | 0.959 |
| ~ Porosity (%) | 10.8 | 7.2 | 6.2 | 6.1 | 6.0 |

## FIGURE CAPTIONS

Figure 1. SENB specimen dimensions (h = thickness: 2, 4, 6, 8 and 10mm).

Figure 2. Analysis of force displacement data (laser sintered specimen of nylon-12).

Figure 3. Energy to initiate crack growth in nylon-12 injection moulded and laser sintered specimens.

Figure 4(a). Positions of DSC samples from laser sintered specimens: cross-sections of 15mm x 2mm and 15mm x 4mm.

Figure 4(b). Positions of DSC samples from laser sintered specimens: cross-sections of 15mm x 6mm, 15mm x 8mm and 15mm x 10mm.

Figure 5(a). DSC curves for samples taken from laser sintered nylon-12 specimen of 15mm by 2mm cross-section.

Figure 5(b). DSC curves for samples taken from laser sintered nylon-12 specimen of 15mm by 10mm cross-section.

Figure 6(a). Corrected force displacement curves for injection moulded PA12 specimens.

Figure 6(b). Corrected force displacement curves for laser sintered PA12 specimens.

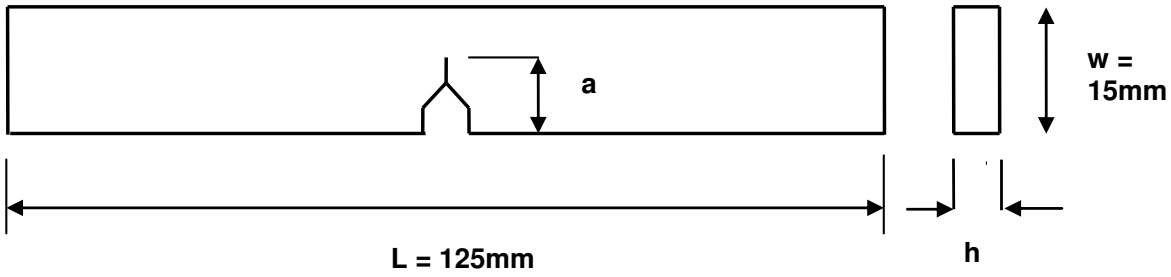


**Figure 1. SENB specimen dimensions (h = thickness: 2, 4, 6, 8 and 10mm).**

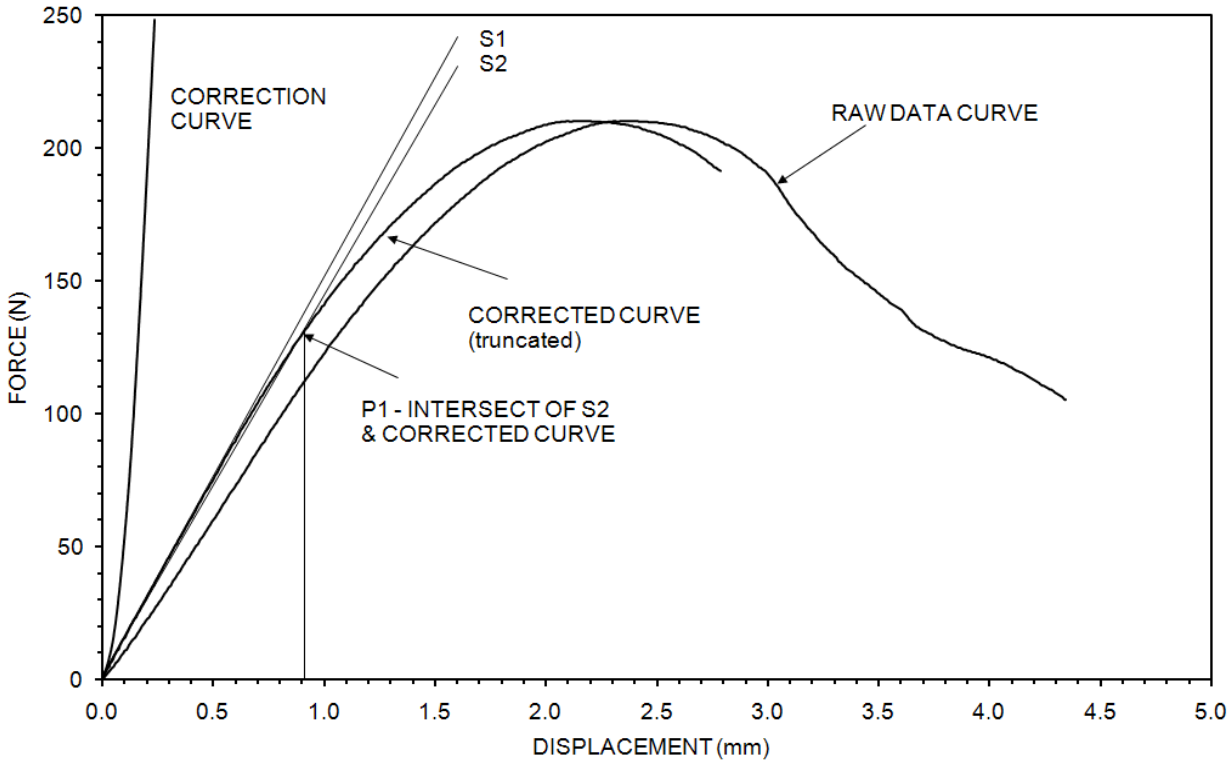


**Figure 2. Analysis of force displacement data (laser sintered specimen of nylon-12).**

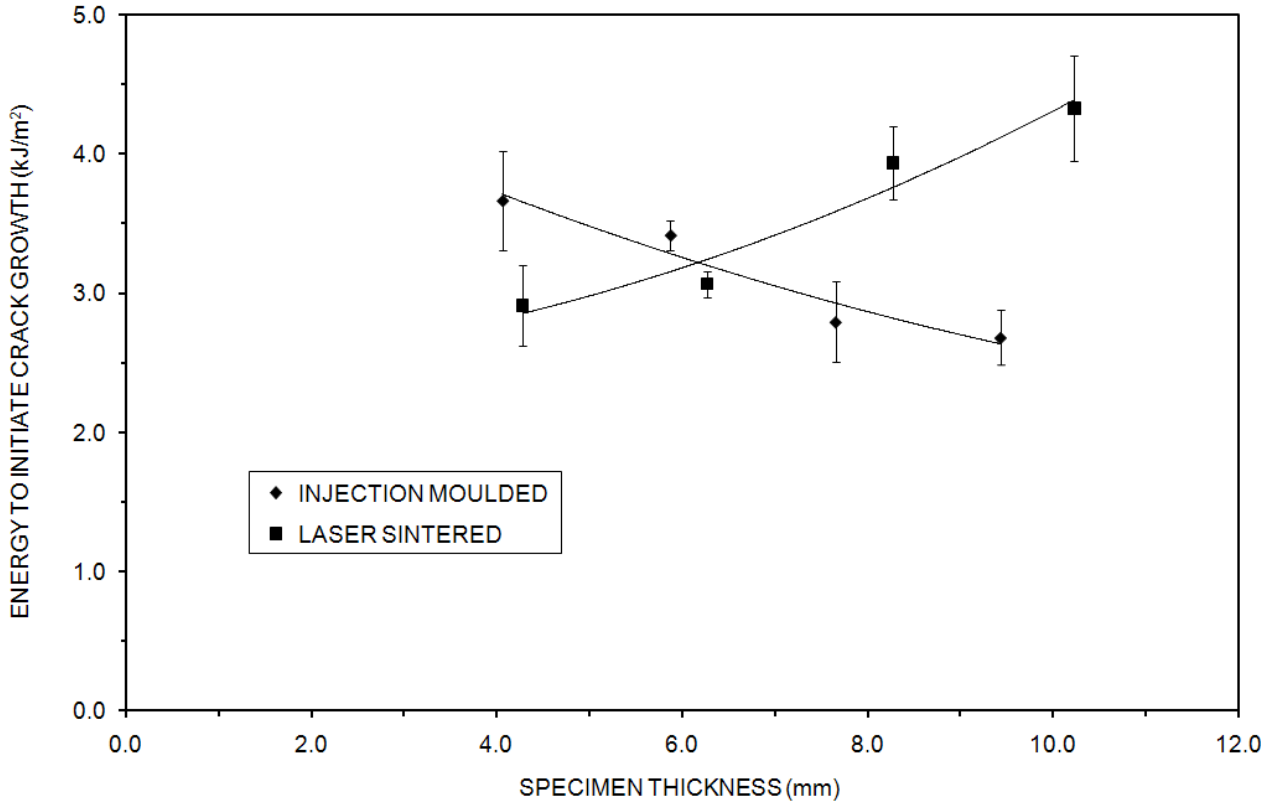


**Figure 3. Energy to initiate crack growth in nylon-12 injection moulded and laser sintered specimens.**

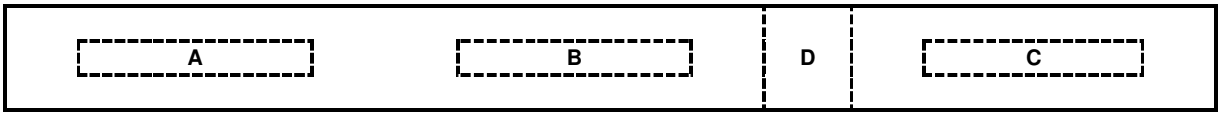


**Figure 4(a). Positions of DSC samples from laser sintered specimens: cross-sections of 15mm x 2mm and 15mm x 4mm.**

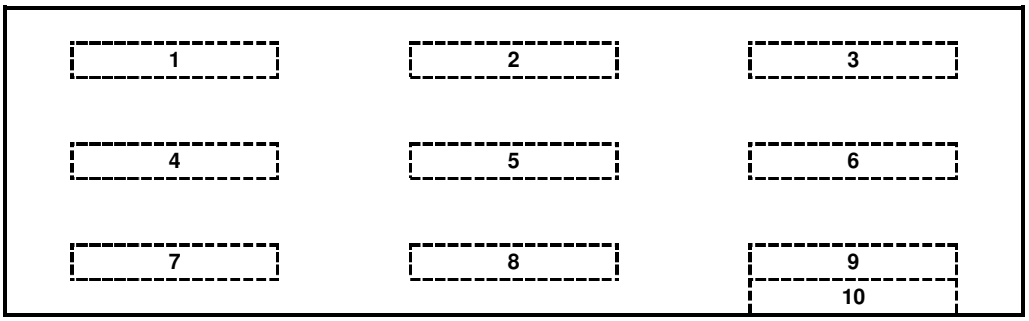


**Figure 4(b). Positions of DSC samples from laser sintered specimens: cross-sections of 15mm x 6mm, 15mm x 8mm and 15mm x 10mm.**

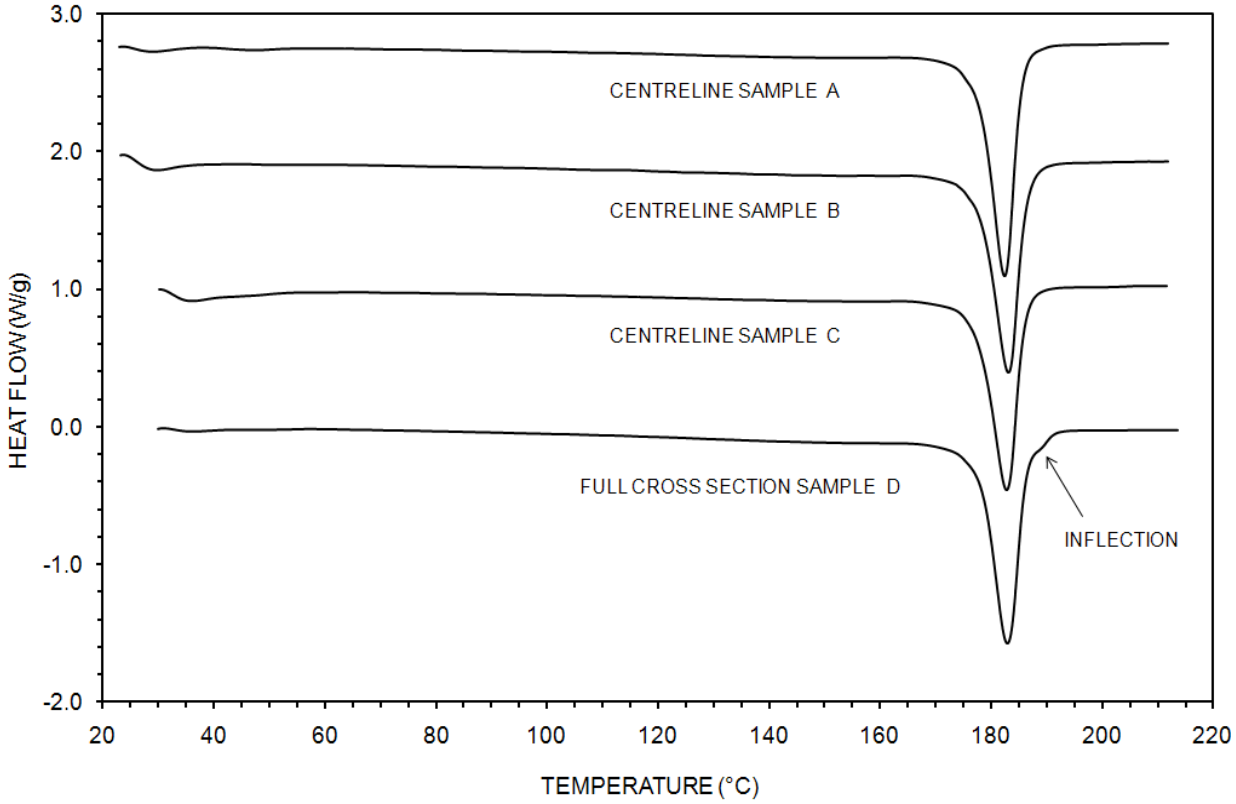


**Figure 5(a). DSC curves for samples taken from laser sintered nylon-12 specimen of 15mm by 2mm cross-section.**

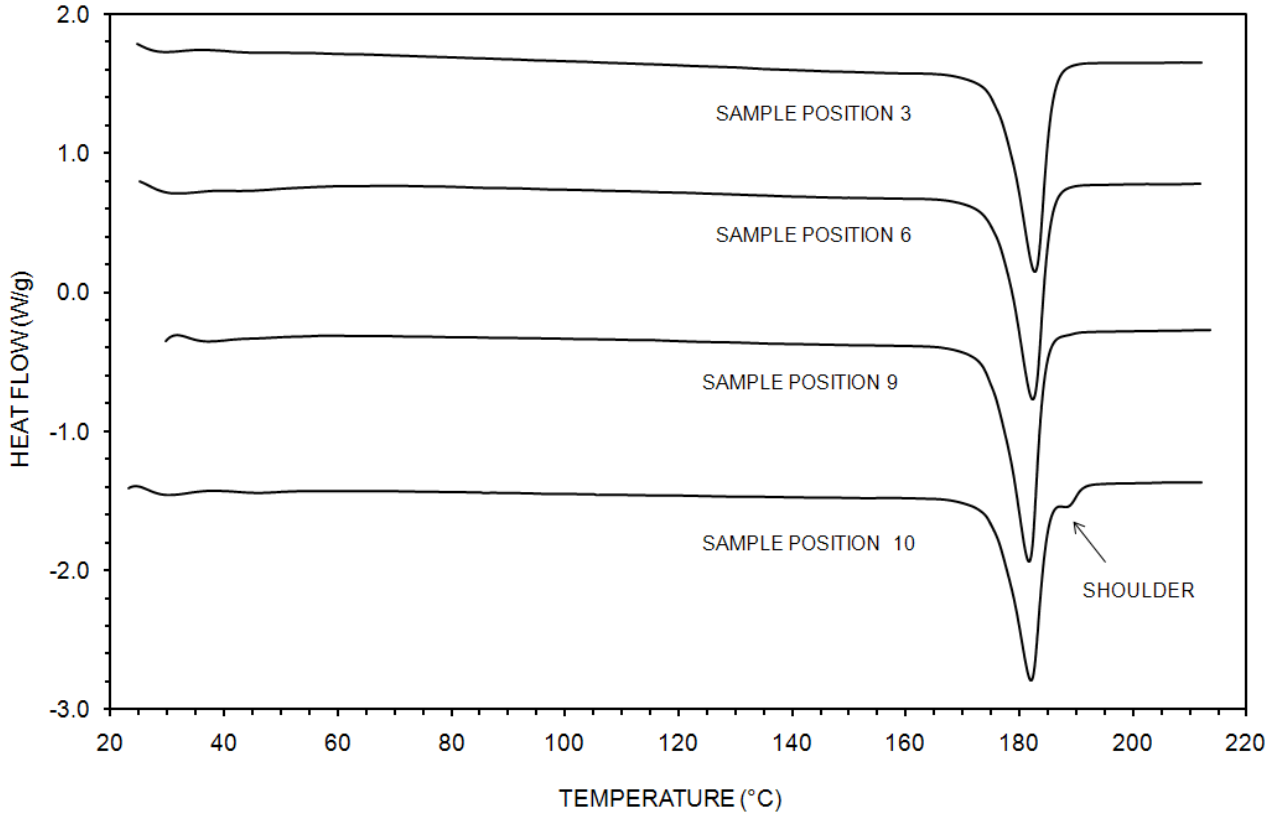


**Figure 5(b). DSC curves for samples taken from laser sintered nylon-12 specimen of 15mm by 10mm cross-section.**

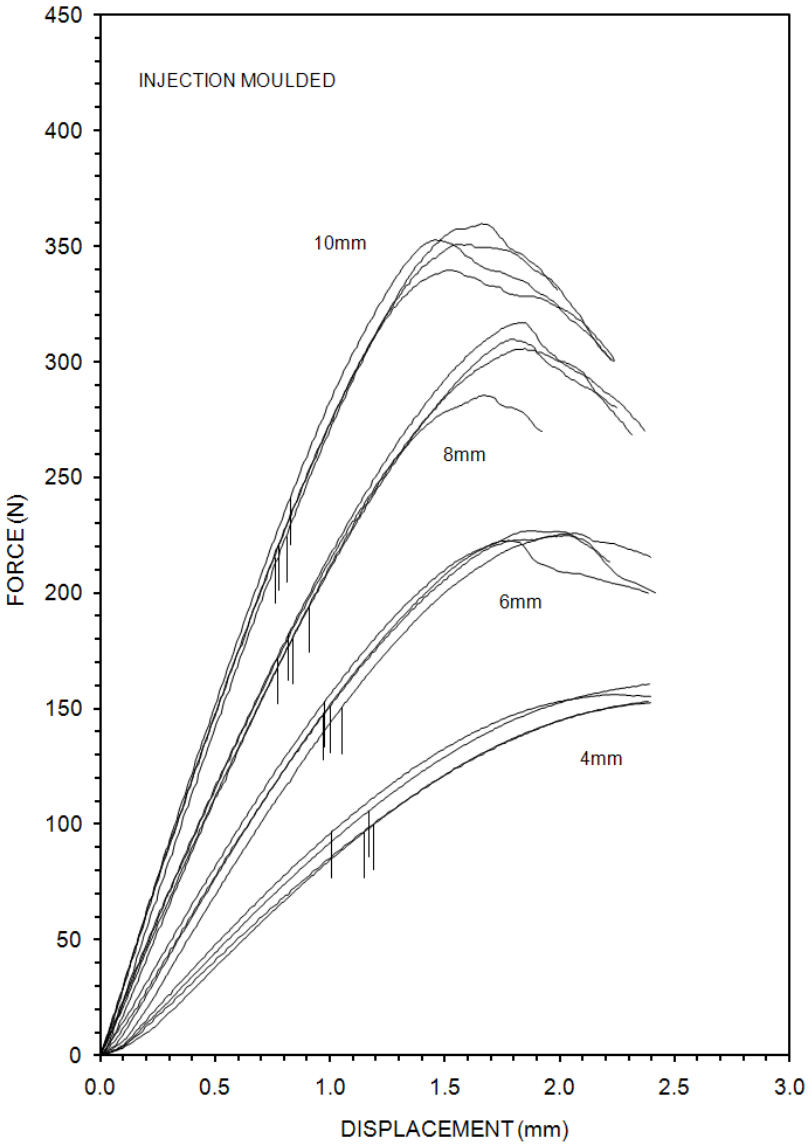


**Figure 6(a). Corrected force displacement curves for injection moulded PA12 specimens.**

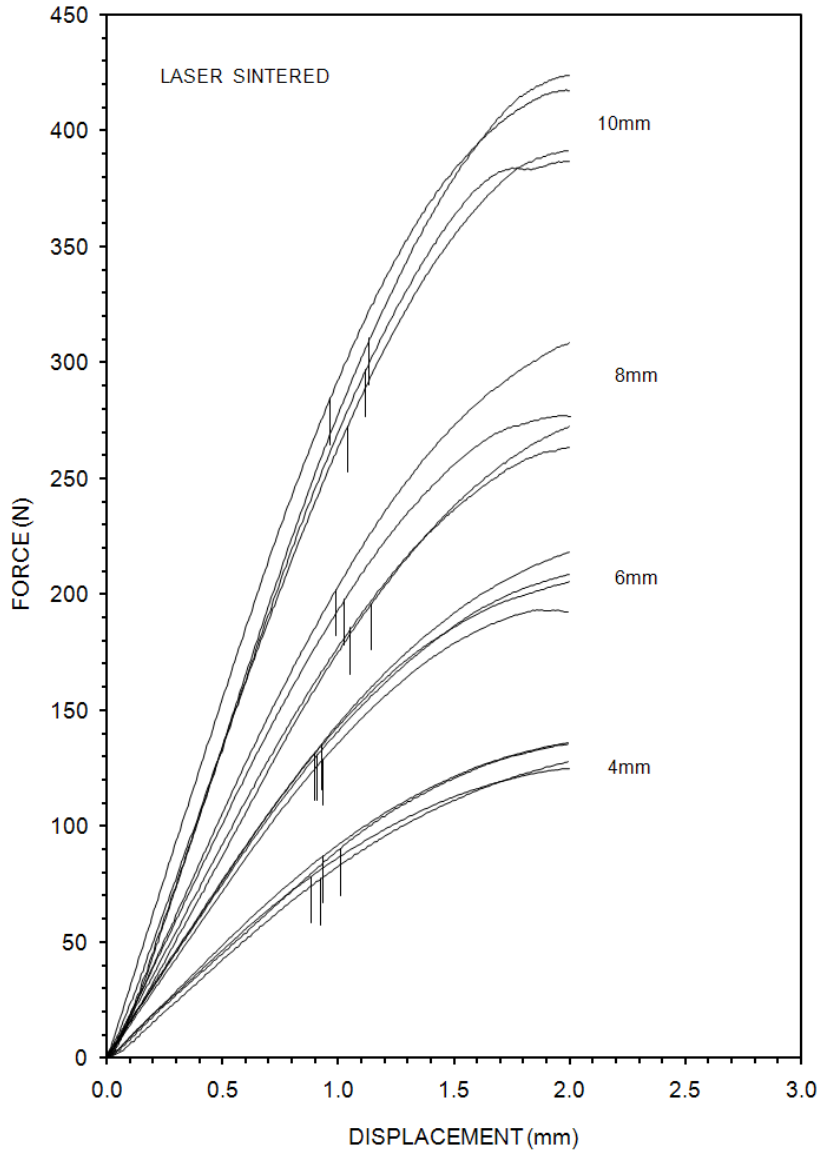


**Figure 6(b). Corrected force displacement curves for laser sintered PA12 specimens.**